EUMETSAT Satellite Application Facility on
Support to Operational Hydrology and Water Management

EUMETSAT H SAF SUPPORT TO OPERATIONAL HYDROLOGY AND WATER MANAGEMENT

Algorithm Theoretical Baseline Document (ATBD) for product H68 (P-IN-PMW)

Gridded MW instantaneous precipitation rate based on inter-calibrated PMW instantaneous precipitation rate estimates

DOCUMENT CHANGE RECORD

Issue / Revision	Date	Authors	Description
1.0	13/12/2019	Leo Pio D'Adderio, Giulia Panegrossi (CNR-ISAC)	Baseline Document
2.0	30/06/2020	Leo Pio D'Adderio, Giulia Panegrossi (CNR-ISAC)	Revised Document
3.0	15/10/2021	Leo Pio D'Adderio, Giulia Panegrossi (CNR-ISAC)	Revised Document

Table of contents

List of Tables

List of Figures

1. Executive summary

The Algorithm Theoretical Baseline Document (ATBD) provides a detailed description of the algorithm used to provide a Level 3 microwave-based (MW-based) precipitation rate product based on the exploitation of all available cross-track and conically scanning passive microwave radiometers, equipped with precipitation sensing channels, on board Low Earth Orbit (LEO) satellites. It is based on instantaneous precipitation rate estimates available from the operational products H01, H02B, H18, and auxiliary modules H-AUX-17, and H-AUX-20, merged and inter-calibrated. The algorithm is implemented in the MATLAB programming language.

2. Introduction

With the aim of providing users with gridded, optimal MW-based products at regular time intervals, the H SAF product portfolio has been enlarged to provide H68 (P-IN-PMW), a Level 3 (gridded) MW-based instantaneous precipitation rate estimate, based on the combination of PMW (PMW) Level 2 instantaneous precipitation rate products. H68 is provided every half hour, on a regular grid at 0.25°x0.25° resolution over the extended H SAF area (LAT 60°S – 75°N, LON 60°W – 60°E). It is obtained from the precipitation rate estimates of the PMW (Level 2) operational products H01 (based on CDRD algorithm for SSMIS radiometers, Casella et al., 2013, Sanò et al., 2013, Mugnai et al., 2013 a,b), H02B (based on PNPR algorithm for AMSU/MHS radiometers, Sanò et al., 2015), and H18 (based on PNPR-V2 algorithm for ATMS radiometer, Sanò et al., 2016), and on the auxiliary modules H-AUX-17 (CDRD-V2 algorithm for AMSR2 radiometer, Casella et al., 2017), and H-AUX-20 (PNPR-V3 algorithm for GMI radiometer, Sanò et al., 2018). All the available overpasses at a given grid-box every 30 minutes by DMSP (SSMIS), MetOp/NOAA (AMSU/MHS), GCOM-W1 (AMSR2), SNPP and NOAA-20 (ATMS) and GPM-Core Observatory (GMI) satellites are considered. The product is provided in NRT, but because of the latency of some of the input products (e.g., as high as 3 hours for H01), the timeliness is set at 4 hours. This means that the product will be made available in the worst case (*at the latest)* 4 hours after sensing. H68 is delivered every half hour (generation frequency) from 00:00 UTC to 23:30 UTC to provide instantaneous precipitation rate in each grid box, where at least one overpass by any of the PMW radiometers cited above is available.

This product will be of interest for applications in hydrology, oceanography, national meteorological services and, in general, for research & development activities by research institutes in Europe and worldwide. The H68 product is mostly aimed at users who need precipitation rate estimates at higher latitudes, where products based on merged MW/IR observations are affected by greater uncertainties related to the slant observations of SEVIRI radiometer. The product is also aimed at users who are interested in MW-based products, and, instead of dealing with the different Level 2 MW precipitation rate products, that might be available at a specific location at a given time (characterized by different orbits, swath sizes, and spatial resolution), prefer or need one "optimal" MW precipitation rate estimate at a given time for a given location. It is worth noting that all international agencies delivering operational PMW precipitation rate products distribute both Level 2 (orbital) and Level 3 (usually daily mean or monthly) products. With H68 product, H-SAF adds a new product very suitable for further processing (e.g., time integration, merging with other observations) to obtain products to be used in hydrological models. The product can be used, for example, to easily derive daily mean (H67) or monthly MW-based precipitation estimates, and to carry out seasonal or inter-annual variability analysis.

For each grid-box at 0.25°x0.25° resolution, every 30 min, H68 provides:

1. Instantaneous precipitation rate (mm/h), where available.
2. Indication of the phase of the precipitation.
3. Quality Index (0-100) of the precipitation rate estimate.
4. Number and type of conical and cross-track satellites overpassing each grid-box in the considered half hour, and their total number.

The statistical score to be used for the accuracy assessment of this product is the same as the one used for the MW level 2 products, i.e., the Fractional Standard Error (FSE) percent. The minimum requirements are FSE = 200% (Threshold), FSE = 150% (Target), FSE = 100% (Optimal) for precipitation rate higher than 1 mmh^{-1}). The FSE is the ratio between RMSE (Root Mean Square Error) and the mean “true” value from the ground measurements used as reference (i.e. meteorological radar and rain gauge over Europe, and GPM DPR over the rest of the coverage area).

3. Architecture of the product generation chain

The architecture of the H68 product generation chain is shown in Figure 1.

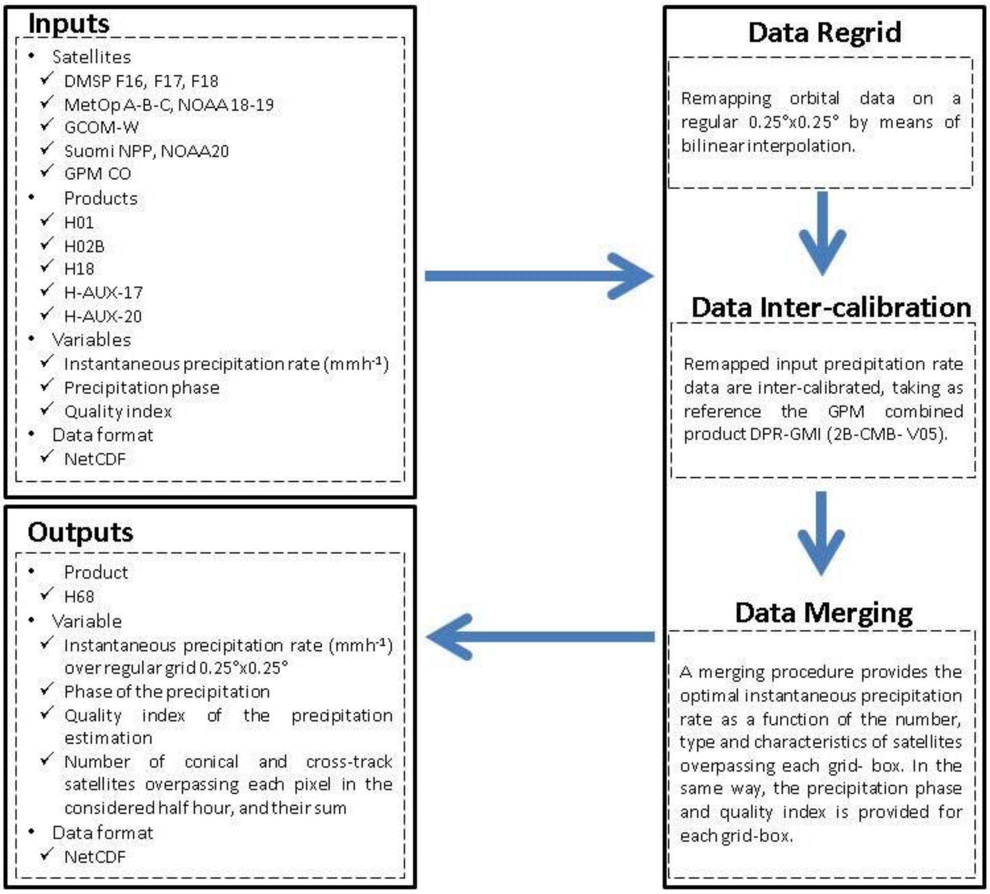

Figure 1: Architecture of H68 product generation chain.

3.1 Algorithm description

The H68 algorithm mainly consists of three modules:

a. remapping module;
b. adjustment module;
c. merging module.

The remapping module makes use of CDO (Climate Data Operator), a collection of command line operators developed to manipulate and analyse Climate and NWP model Data. More information about CDO can be found in [1]. The remapping module performs bilinear interpolation of the instantaneous precipitation rate in the original orbital (irregular) grid to remap them on a regular grid. The target (regular) grid description is given as an external file. The scheme used in CDO considers a local bilinear approximation to interpolate to a point in a quadrilateral grid. For the extended H SAF area at 0.25°x0.25° the grid description file is described below:

Full Disk Grid:
gridtype = lon/lat
xsize = 480
ysize = 540
x_rst = -59.875
xinc = 0.25
y_rst = -59.875
yinc = 0.25

The remapping module runs every 30 minutes, looks for files produced by H01, H02, H18, H-AUX-17, and H-AUX-20 in the last 30 minutes and performs remapping of those files.

The adjustment module runs after the remapping module (i.e. every 30 minutes) and adjusts all the data produced by H01, H02, H18, H-AUX-17, and H-AUX-20 in the previous 30 minutes and remapped over the 0.25°x0.25° grid. The adjustment is performed by taking as reference the precipitation rate estimate provided by the GPM GMI-DPR combined product (2B-CMB V05) over the extended H SAF area (LAT 60°S – 75°N, LON 60°W – 60°E) from 2014 to 2018. For each Level 2 PMW product (i.e. H01, H02, H18, H-AUX-17, and H-AUX-20) all grid boxes where coincident observations between each radiometer and the GPM GMI/DPR are available are considered. The GPM 2B-CMB estimates and the Level 2 PMW estimates are compared to derive the coefficients *a* and *b* of a power-law fit by considering the five-years long coincidence dataset. The power law fit is described as follows:

$$PR_{adj} = a \cdot PR^b$$

where PR_{adj} is the gridded adjusted precipitation rate and PR is the gridded precipitation rate for each H68 input product (i.e. H01, H02, H18, H-AUX-17, and H-AUX-20.

The results of the comparison between the different Level 2 products and the GPM product, have evidenced that different calibration is needed for all products for the different surface types (e.g. ocean and land/coast), except for H-AUX-17 (AMSR2 product) and H-AUX-20 (GMI product) where the calibration is carried out only over ocean. Furthermore, the adjustment is not applied to the whole range of precipitation intensity estimated by the different products. Table 1 reports for each product (i.e. H01, H02, H18, H-AUX-17, and H-AUX-20) the coefficient *a* and *b* (whenever they are derived) and the precipitation rate range in which the power law is applied.

Product	Surface/Region	*a*	*b*	Range (mmh^{-1})
H01	Ocean/Africa	1.00	0.73	0.1-100
	Land/Africa	1.00	0.69	0.1-100
	Ocean/"Europe"	1.34	0.58	0.1-100
	Land/"Europe"	1.15	0.67	0.1-100
H02B	Ocean/Africa	1.19	0.62	0.1-100

	Land/Africa	1.15	0.56	0.1-100
	Ocean/"Europe"	1.11	0.68	0.1-100
	Land/"Europe"	1.37	0.60	0.1-100
H18	Ocean	1.22	0.73	0.1-100
	Land	1.42	0.66	0.1-100
H-AUX-17	Ocean	0.22	1.62	0.1-100
	Land	/	/	/
H-AUX-20	Ocean	1.28	0.96	0.1-10
	Ocean	0.33	1.43	10-100
	Land	/	/	/

Table 1: coefficients *a* and *b* and range of application of the power law derived for each input's product of H68. The power law fits are derived for different surface type. Only for H01 and H02B they are derived separately above 35°N and below 35°S ("Europe"),and between 35° N and 35° S ("Africa"). Two different power laws (applied to different precipitation rate ranges) are derived over Ocean for H-AUX-20.

The merging module runs after the calibration module (i.e. every 30 minutes) and performs an ensemble mean of all the data produced by H01, H02, H18, H-AUX-17, and H-AUX-20 in the previous 30 minutes and remapped at 0.25°x0.25° and calibrated. The ensemble mean module is organized as follow:

1. Two separate rankings based on the MW radiometer characteristics, one for the products based on conical scanning radiometers, and one for the products based on cross-track scanning radiometers, are derived. The rankings, which take into account the characteristics of the sensors and the pixel-based quality flag associated, are defined as follows:

Conical Satellites	**Cross-track Satellites**
1. H-AUX-20 (GMI)	1. H18 (ATMS-NPP)
2. H-AUX-17 (AMSR2)	2. H18 (ATMS-NOAA20)
3. H01 (F17)	3. H02B (MHS-MetOp B)
4. H01 (F18)	4. H02B (MHS-NOAA18)**
5. H01 (F16)	6. H02B (MHS-NOAA19)
	7. H02B (MHS-MetOp A)
	8. H02B (MHS MetOp C)

*Table 2: conical and cross-track satellite ranking. ** MHS onboard NOAA-18 is no longer available, but it is considered in the Table for possible re-processing.*

2. The MW precipitation products available over each grid-box in the considered half hour are sorted according to the rankings of Table 2.
3. The two best MW precipitation products (one for conical and one for cross-track, if available, following then the rankings in Table 1) are averaged to provide the "optimal" instantaneous precipitation estimate for each grid-box. In the same way, the precipitation phase associated to the MW input products used (i.e. H01, H02, H18, H-AUX-17 and H-AUX-20) is averaged to provide the precipitation phase over each grid-box. On the other hand, the quality index is set equal to the quality of the worst of the two input products.

3.2 Input files

Each input file contains latitude, longitude, time, instantaneous precipitation rate (units mm h^{-1}), phase, quality index and a surface type index produced by H01, H02, H-AUX-17, H18 and H-AUX-20. The general format of an input file name is the following:

<Algorithm> <Date> <StartTime> <EndTime> <Satellite> <IdNumber>.Extension

where

1. Algorithm is one among H01, H02, H-AUX-17, H18 and H-AUX-20;
2. Date contains a four-digit year, a two-digit month, and a two-digit day (YYYYM-MDD);
3. StartTime contains a two-digit hour and a two-digit minute (HHMM), which indicates the time corresponding to the first pixel within the H-SAF area, as reported in the file. Hours are presented in a 24-hour time format, with 00 indicating midnight. All times are in Coordinated Universal Time (UTC);
4. EndTime contains a two-digit hour and a two-digit minute (HHMM), which indicates the time corresponding to the last pixel within the H-SAF area, as reported in the file. Hours are presented in a 24-hour time format, with 00 indicating midnight. All times are in Coordinated Universal Time (UTC); ***at the moment, only H-AUX-20 reports the EndTime in the file name.***
5. Satellite is DMSP F16, F17, F18 for H01; NOAA18, NOAA19, MetOpA, MetOpB, MetOpC for H02B; GCOM-W1 for H-AUX-17; Suomi NPP and NOAA20 for H18; GPM CO for H-AUX-20
6. IdNumber contains a five-digit number (a seven-digit number for MHS and six-digit number for GMI) related to orbit number as classified by NOAA/GPM CLASS convention;
7. Extension is nc (netcdf 4).

Example:
h01_20141009_0029_DMSP16_56623_rom_0.25.nc
h02_20141009_0022_NOAA19_2920506_0.25.nc
H-AUX-17_20141009_0128_GCOM-W1_12738_0.25.nc
h18_20141009_0048_NPP_15275_0.25.nc
H-AUX-20_20141009_0012_GMI_003475_0.25.nc

3.3 Output files

The output file format is NetCDF. Each output file is generated every half hour, and it contains regular grid matrices of latitude, longitude, instantaneous precipitation rate, phase, quality index, flags indicating the number and types of radiometers available in each grid point, and the total number of overpasses available.

Dimension definitions:

- nlat: 540 (Number of 0.25° grid intervals of latitude from 75°N to 60°S).
- nlon: 480 (Number of 0.25° grid intervals of longitude from 60°W to 60°E).

Variable definitions (provided in each grid point):

- rr: precipitation rate in mm/h for each grid point
- TotalCount: number of available PMW (both conical and cross-track) overpasses
- CrossTrackCount: number of available conical PMW overpasses
- ConicalCount: number of available cross-track PMW overpasses
- IdSensorBin: binary variable identifying each type of satellite/sensor available
- phase: precipitation phase

- qind: quality index of the precipitation estimation
- lat: latitude of each grid point
- lon: longitude of each grid point

The general format of output file names is the following:
<Algorithm> <Id> <Date> <StartTime> <EndTime>.Extension where

1. Algorithm is H68;
2. Date contains a four-digit year, a two-digit month, and a two-digit day (YYYYMMDD);
3. StartTime contains a two-digit hour, two-digit minute and a two-digit second (HHMMSS), which indicates the starting hour, minute (00 or 30) and second (00) of the considered half hour;
4. EndTime contains a two-digit hour, two-digit minute and a two-digit second (HHMMSS), which indicates the ending hour, minute (29 or 59) and second (59) of the considered half hour;
5. Extension is nc (netcdf 4).

Example:
h68_ 20170101_000000_002959.nc
h68_ 20170101_003000_005959.nc

4. Example of H68 product

The advantage of combining five different precipitation estimates (i.e. H01, H02, H18, H-AUX-17 and H-AUX-20) stems mainly from the high temporal sampling of the precipitation when observations from all available cross-track and conical scanning radiometers are considered. In particular, the adopted methodology allows to take into account the characteristics of the different instruments (i.e. conical and cross-track), calibrate and combine the different, multiple estimates available at a given location, and to provide the users with one unique MW-.based precipitation rate estimate over a regular grid.

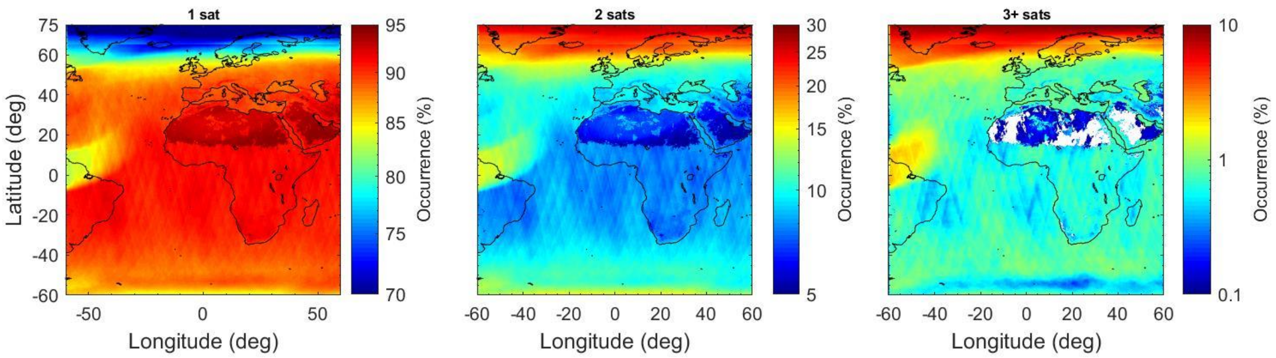

Figure 2: Mean probability to have only one, two and three or more satellite overpasses in each grid-box in 30 minutes by considering two years of data. Only overpasses relative to valid Level 2 precipitation rate products are shown (e.g., H-AUX-17 from AMSR2 is flagged over land/desert for low values of quality index).

The mean probability showed in Figure 2 is obtained considering only overpasses relative to valid Level 2 precipitation rate products are shown (e.g., H-AUX-17 from AMSR2 is flagged over land/desert for low values of quality index) leading to have lower occurrence of two or more overpasses over desert (e.g. Sahara region and Arabic Peninsula). The probability to have two or more overpasses in 30 minutes increases moving away from the inter-tropical region towards the high latitude region. At the mid-latitude, the probability to have three or more overpasses over each grid box is around 1%.

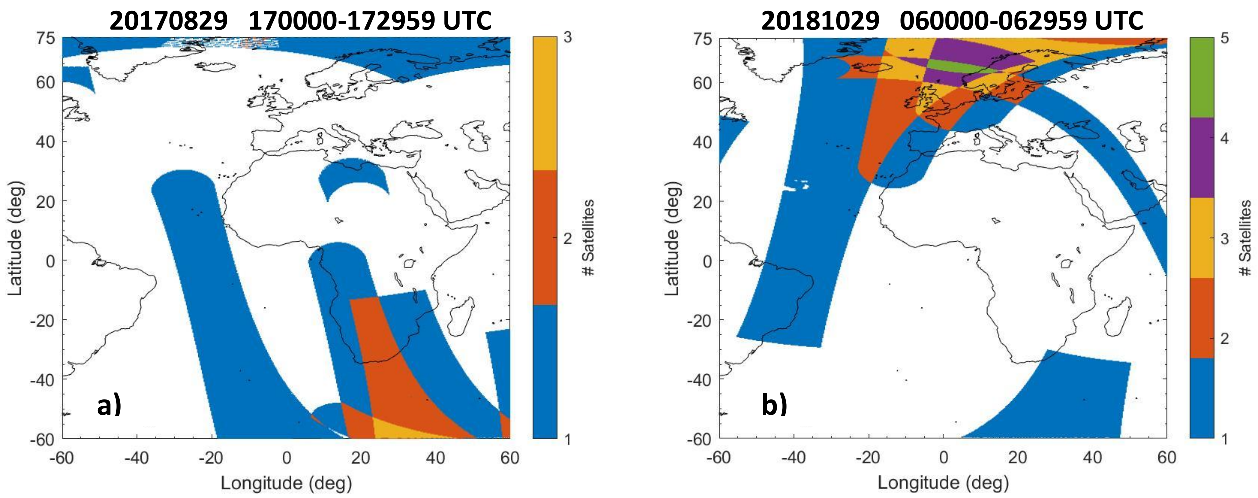

Figure 3: Example of number of overpasses for each grid-box for two different half-hour. a) is referred to the case of 29th August, 2017 between 170000 and 172959 UTC, b) is referred to the case of 29th October, 2018 between 060000 and 062959 UTC.

Figure 3 shows, as an example, the snap-shot of the number of the satellite overpasses over each 0.25°x0.25° grid box for two different cases considering a given half-hour. The high latitudes present the possibility to have up to five simultaneous satellite measurements in a given half-hour interval (i.e. green area in Figure 3b). At the same time, it is worth noting that there are some regions (i.e. the white areas in Figures 3) without any MW radiometer

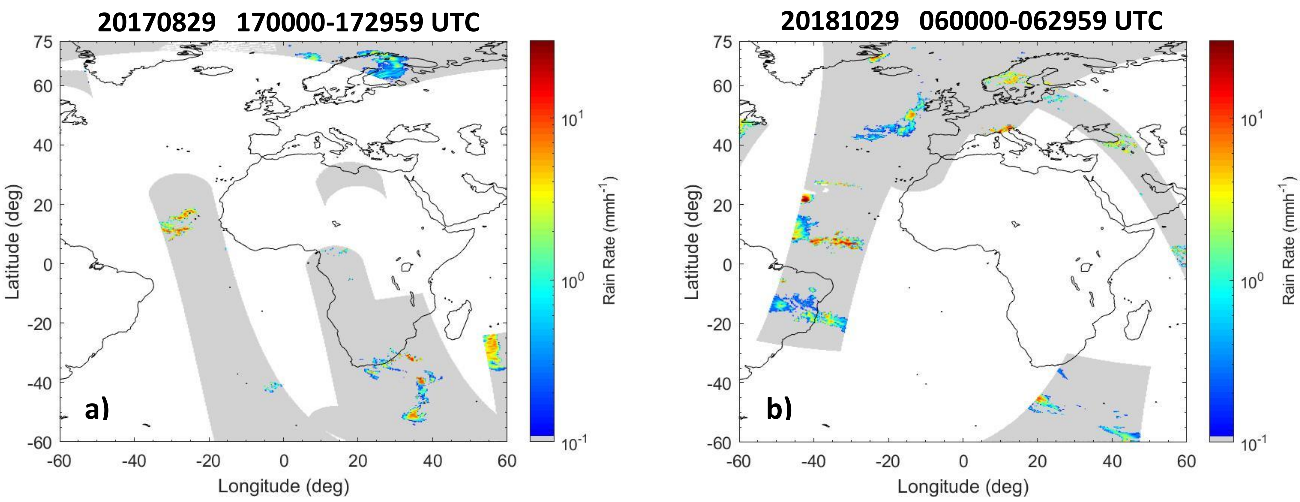

Figure 4: Precipitation estimates for two different half-hour intervals. a) is referred to the case of 29th August, 2017 between 170000 and 172959 UTC, b) is referred to the case of 29th October, 2018 between 060000 and 062959 UTC.

overpass available in the considered half-hour interval. It is worth noting that the Figure 3 has to be coupled with Figure 2 highlighting that even if situations shown in Figure 3 (especially Figure 3b) are possible, their occurrence probability is rather low. Figure 4 shows the precipitation estimation corresponding to the measurements collected in the half-hour interval shown as example in Figure 3. The grey parts in both Figure 4a and 4b correspond to the grid-boxes where the precipitation rate = 0 mm h^{-1}, even if a MW radiometer overpass is available. Figure 4 evidences the usefulness of H68 product, which combines and remaps over a regular grid all the PMW measurements available, providing the best possible precipitation rate estimation.

5. Application of H68 product

H68 half-hour instantaneous precipitation rate allows to cover the so called extended H SAF area (i.e. LAT 60°S – 75°N, LON 60°W – 60°E) every 30 minutes, thanks to the frequent overpasses from the constellation of PMW radiometers. Furthermore, with respect to rain gauge or ground-based radar network, provides precipitation rate estimation also over ocean. In this Section, an application relative to a great storm hitting the whole Italian peninsula on 29th October, 2018, is discussed.

Figure 5 shows the mean precipitation rate as estimated by H68 (Figure 5a) and as estimated by the Italian rain gauge network provided by the Civil Protection Department and interpolated using the GRISO technique (Pignone et al. 2010; Feidas et al. 2018) (Figure 5b) between 130000 and 135959 UTC of 29th October, 2018. The pattern agreement between H68 and GRISO is good, while a slight overestimation is evident over the Tyrrhenian coast (even though the GRISO interpolation may be affected by the lack of rain gauge stations over the sea). Figure 5 shows also the potential of H68, highlighting the precipitation over the sea between Sicily and southern Lazio and off the coast, and its limitation in providing the light, orographic precipitation over Piedmont, in Northwest Italy, due to the lack of MW radiometer overpasses(white area in Figure 5a) in the half hour intervals considered.

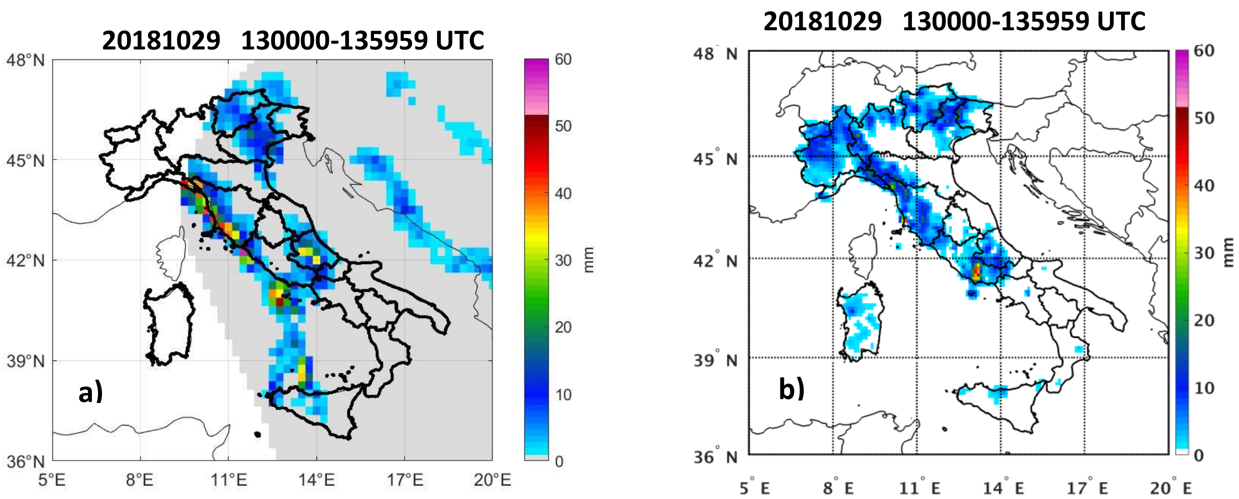

Figure 5: Hourly mean precipitation rate as a) estimated by H68 and b) by GRISO for the time interval 130000-135959 UTC for 29th October, 2018 case.

6. References

1. Casella, D., Panegrossi, G., Sanò, P., Mugnai, A., Smith, E.A., Tripoli, G.J., Dietrich, S., Formenton, M., Di Paola, F., Leung, H. W.-Y., and Mehta, A.V.: Transitioning from CRD to CDRD in Bayesian retrieval of rainfall from satellite passive microwave measurements, Part 2: Overcoming database profile selection ambiguity by consideration of meteorological control on microphysics, IEEE Trans. Geosci. Remote Sens, vol.51, no.9, pp.4650-4671, 2013, DOI: 10.1109/TGRS.2013.2258161, 2013.
2. Casella D., Casella D., L. M. Amaral, S. Dietrich, A. C. Marra, P. Sanò, and G. Panegrossi, The Cloud Dynamics and Radiation Database algorithm for AMSR2: exploitation of the GPM observational dataset for operational applications, IEEE J. of Sel. Topics in Appl. Earth Obs. and Rem. Sens. (J-STARS), 10(*8), DOI :* 10.1109/JSTARS.2017.2713485*, 2017*.
3. CDO website at <https://code.zmaw.de/projects/cdo>.
4. Feidas, H., F. Porcù, S. Puca, A. Rinollo, C. Lagouvardos, and V. Kotroni, 2018: Validation of the H-SAF precipitation product H03 over Greece using rain gauge data. Theor. Appl. Climatol., 131, 377–398, https://doi.org/10.1007/s00704-016-1981-9.
5. Mugnai, A., Casella, D., Cattani, E., Dietrich, S., Laviola, S., Levizzani, V., Panegrossi, G., Sanò, P., Biron, D., De Leonibus, L., Melfi, D., Rosci, P., Vocino, A., Zauli, F., Puca, S., Rinollo, A., Milani, L., Porcù, F., and Gattari, F.: Precipitation products from the Hydrology SAF, Nat. Hazards Earth Syst. Sci., 13, 1959-1981, DOI: 10.5194/nhess-13-1959-2013, 2013a.
6. Mugnai A., E. A. Smith, G. J. Tripoli, B. Bizzarri, D. Casella, S. Dietrich, F. Di Paola, G. Panegrossi, P. Sanò, CDRD and PNPR Satellite Passive Microwave Precipitation Retrieval Algorithms: EuroTRMM / EURAINSAT Origins and H-SAF Operations, Nat. Hazards Earth Syst. Sci., 13, 887-912, 2013b.
7. Pignone, F., N. Rebora, F. Silvestro, and F. Castelli, 2010: GRISO (Generatore Random di Interpolazioni Spaziali da Osservazioni incerte)-Piogge. Rep. 272/2010, 353 pp.
8. Sanò, P., Casella, D., Mugnai, A., Schiavon, G., Smith, E. A., and Tripoli, G. J.: Transitioning from CRD to CDRD in Bayesian retrieval of rainfall from satellite passive microwave measurements: Part 1. Algorithm description and testing, IEEE T. Geosci. Remote, 51, 4119–4143, 2013.
9. Sanò, P., Panegrossi, G., Casella, D., Di Paola, F., Milani, L., Mugnai, A., Petracca, M., and Dietrich, S.: The Passive microwave Neural network Precipitation Retrieval (PNPR) algorithm for AMSU/MHS observations: description and application to European case studies, Atmos. Meas. Tech., 8, 837-857, DOI:10.5194/amt-8-837-2015, 2015.
10. Sanò, P., Panegrossi, G., Casella, D., Marra, A. C., Di Paola, F., and Dietrich, S.: The new Passive microwave Neural network Precipitation Retrieval (PNPR) algorithm for the cross-track scanning ATMS radiometer: description and verification study over Europe and Africa using GPM and TRMM spaceborne radars, Atmos. Meas. Tech., 9, 5441-5460, doi:10.5194/amt-9-5441-2016, 2016.
11. Sanò P., G. Panegrossi, D. Casella, A. C. Marra, L. P. D'Adderio, J.-F. Rysman, S. Dietrich, The Passive Microwave Neural Network Precipitation Retrieval (PNPR) algorithm for the Conical Scanning GMI Radiometer, Remote Sens. 10, 1122; doi:10.3390/rs10071122, 2018